Biodegradation (2012) 23:189–198
DOI 10.1007/s10532-011-9498-5

ORIGINAL PAPER

Integrated photocatalytic-biological reactor for accelerated 2,4,6-trichlorophenol degradation and mineralization

Yongming Zhang · Xia Sun · Lujun Chen · Bruce E. Rittmann

Received: 25 March 2011 / Accepted: 30 June 2011 / Published online: 13 July 2011

Abstract An integrated photocatalytic-biological reactor (IPBR) was used for accelerated degradation and mineralization of 2,4,6-trichlorophenol (TCP) through simultaneous, intimate coupling of photocatalysis and biodegradation in one reactor. Intimate coupling was realized by circulating the IPBR's liquid contents between a TiO_2 film on mat glass illuminated by UV light and honeycomb ceramics as biofilm carriers. Three protocols—photocatalysis alone (P), biodegradation alone (B), and integrated photocatalysis and biodegradation (photobiodegradation, P&B)—were used for degradation of different initial TCP concentrations. Intimately coupled P&B also was compared with sequential P and B. TCP removal by intimately coupled P&B was faster than that by P and B alone or sequentially coupled P and B. Because photocatalysis relieved TCP inhibition to biodegradation by decreasing its concentration, TCP biodegradation could become more important over the full batch P&B experiments. When phenol, an easy biodegradable compounds, was added to TCP in order to promote TCP mineralization by means of secondary utilization, P&B was superior to P and B in terms of mineralization of TCP, giving 95% removal of chemical oxygen demand. Cl^- was only partially released during P experiments (24%), and this corresponded to its poor mineralization in P experiments (32%). Thus, intimately coupled P&B in the IPBR made it possible obtain the best features of each: rapid photocatalytic transformation in parallel with mineralization of photocatalytic products.

Keywords Photocatalysis · Biofilm · Reactor · Trichlorophenol · Biodegradation

Y. Zhang (✉) · X. Sun
Department of Environmental Engineering, College of Life and Environmental Science, Shanghai Normal University, Shanghai 200234, People's Republic of China
e-mail: zhym@shnu.edu.cn

L. Chen
School of Environment, Tsinghua University, Beijing 100084, People's Republic of China

B. E. Rittmann
Swette Center for Environmental Biotechnology, Biodesign Institute, Arizona State University, Tempe, AZ 85287-5701, USA

Introduction

Trichlorophenol (TCP) has been used widely as a pesticide, herbicide, and lumber antimicrobial during the last century (Häggblom 1992). In addition, TCP also is a byproduct from industrial processes, especially the bleaching of pulp and paper (Ali and Sreekrishnan 2001). The widespread use of TCP has led to its presence in the natural environment, creating a potential human-health risk. Prolonged

occupational exposure to TCP can induce cancer, and TCP has been shown to be carcinogenic in rats and mice (National Cancer Institute (NCI) 1979). TCP metabolites also may induce mutations in double-stranded DNA (Juhl et al. 1991). The World Health Organization assigns a maximum admissible concentration of 200 μg/l for TCP in drinking water (Chu and Wong 2003).

TCP also is inhibitory to microorganisms (Marsolek and Rittmann 2007), and this has precluded its biodegradation in normal biological wastewater treatment. To overcome this problem, pre-treatment with advanced oxidation processes (AOPs) has been proposed as a means to transform TCP into biodegradable or less-toxic organic compounds. Among the AOPs, one of the most promising is TiO_2 used as a photocatalyst together with UV light (Han et al. 2004; Agrios et al. 2004; Aguedach et al. 2005; Parra et al. 2002; Stafford et al. 1997). When valence-band electrons in TiO_2 absorb UV light, they are excited to the conduction band, which also forms electron–hole pairs. The conduction-band electrons and holes can migrate to the catalyst surface, where they can participate in redox reactions with compounds adsorbed on the photocatalyst or with H_2O. In general, the holes oxidize H_2O to hydroxyl radicals (HO•), which can oxidize organics, or participate in direct electron transfer from an adsorbed species (Stafford et al. 1994).

Although photocatalysis is effective for doing one or a few steps of transformation, it is not efficient for complete mineralization (Chan et al. 2004). A current approach is to follow photocatalyic degradation of TCP with biodegradation in order to allow complete mineralization. This approach is called sequential coupling and is carried out in separate units (Hess et al. 1998; Zhang et al. 2002; Mohanty et al. 2005; Marsolek 2005).

Due to the indiscriminate nature of photocatalytic AOP reactions, sequential coupling has not been easy to implement in a practical setting. The photocatalytic products are many, and some may be inhibitory, difficult to biodegrade, or more oxidized than necessary to make them biodegradable, which wastes oxidant (Marsolek et al. 2008). A more efficient approach would be to have the microorganisms biodegrade transformation products as soon as biodegradable products are generated by photocatalysis. Then, biodegradable products would not be over-transformed, while recalcitrant products could continue to be transformed until they are biodegradable. This approach—having the microorganisms simultaneously on hand to biodegrade the biodegradable products as soon as they are generated—is called *intimate coupling* (Marsolek et al. 2008). With intimate coupling in one reactor, the recalcitrant contaminant can be fully mineralized, but with photocatalyis only responsible for the minimum number of initial transformation steps.

An apparent problem with intimate coupling is that the hydroxyl radicals and the UV light will harm microorganisms unless the microorganisms are protected from them. Marsolek et al. (2008) solved the intimate coupling dilemma by having the microorganisms inhabit the interior of macroporous carriers inside a circulating bed bioreactor; this system is called the photocatalytic circulating-bed biofilm reactor, or PCBBR. Being inside the circulating carriers shaded the microorganisms from UV light and protected them from HO• radicals, which could not penetrate far into the carriers.

Another approach for intimate coupling is the integrated photocatalytic-biological reactor, or IPBR (Zhang et al. 2010a). In the IPBR, biofilm is protected from hydroxyl radicals and UV light by separating phototransformation and biodegradation into two zones that are connected by internal circulation. Zhang et al. (2010a) demonstrated the IPBR concept with phenol photocatalysis and biodegradation.

Here, the IPBR concept is tested using 2,4,6-TCP, a much more recalcitrant model compound than phenol. In particular, sequentially and intimately coupled photocatalysis and biodegradation are compared in order to investigate the hypothesis that intimate coupling is more efficient for accelerated TCP degradation and mineralization. In one set of experiments, the ability to increase the volumetric removal rates is investigated by increasing the influent TCP concentration. In some experiments, phenol, a readily biodegradable aromatic compound, is added in order to enhance the mineralization of TCP and its photocatalysis products by means of secondary utilization (Aranda et al. 2003; Namkung and Rittmann 1987a; Namkung and Rittmann 1987b), in which the utilization of phenol supports the growth of more biomass able to biodegrade TCP.

Materials and methods

Chemicals and materials

2,4,6-TCP was purchased from the Shanghai Sinopharm Chemical Reagent Co., Ltd. Titanium(IV) *n*-butoxide from Yonghua Fine Chemicals Co., Ltd. in Jiangsu province of China was used for making TiO_2 film. The chemicals were all analytical reagent. Mat glass was cut at a glass shop from scrap glass (44 × 60 mm) to be used as the TiO_2-film carrier. A ceramic honeycomb material obtained from the Pingxiang Sanyuan Ceramic Plant was used as the biofilm carrier in the IPBR. The same kind of ceramic honeycomb carrier was used previously for biofilm biodegradation of phenol, 2,4-dichlorophenol, and quinoline (Zhang et al. 2010a; Zhang et al. 2010b; Zhang et al. 2004; Zhang et al. 2002).

Preparation of the TiO_2 film

The mat glasses were coated with a TiO_2 film as reported by Zhang et al. (2010a). X-ray analysis indicated that the coated TiO_2 was anatase (Zhang et al. 2010a).

Integrated photocatalytic-biological reactor (IPBR)

The IPBR was made of polymethyl methacrylate with a working volume of 110 ml, and its configuration is shown in Fig. 1. The reactor was divided into two zones, with the glass with TiO_2 film (the photocatalytic zone) above the glass and biological degrading zone under the glass. The ratio between two zones volume was 1:3, and the retention time in the ceramic carrier was as three times that of the photocatalytic zone. The reactor was open, and the solution was circulated and actively mixing with the circulating pump that had a 30 ml/min flow rate during the operation. The system could be operated in three different modes. When the UV light was turned off and the ceramic honeycomb carrier had biofilm, biodegradation was the lone process for degrading TCP. When the UV light was turned on and the ceramic honeycomb carrier had no biofilm, only photodegradation was possible. Photobiodegradation could occur when the UV light was turned on and the ceramic carrier had biofilm. The reactor was operated in batch mode in all cases.

Acclimation and incubation of TCP-degrading bacteria

Activated sludge was obtained from the underflow of a secondary clarifier at the Longhua municipal wastewater treatment plant in Shanghai. It was acclimated by adding phenol to an inorganic salts medium at 20–25°C for 10 days by replacing the solution every 2 days. The inorganic salts were: ammonium sulfate, 0.1 g/l; potassium dihydrogen phosphate, 0.5 g/l; disodium hydrogen phosphate, 0.5 g/l; magnesium sulfate, 0.5 g/l; and yeast extract, 0.02 g/l. After 3 weeks, phenol was replaced by 2,4,6-TCP. The inorganic salts medium was the same and replaced every day. The concentration of 2,4,6-TCP was increased gradually from 5 to 30 mg/l during acclimation over 20 days.

After 20 days, the ceramic honeycomb carrier was immersed into the acclimated sludge solution for 24 h, allowing the microorganisms to attach to the carrier surface, and then the carrier with microorganisms was moved into the IPBR. In the IPBR, the TCP and inorganic salts solution was fed to let a stable biofilm form on the surface of the carrier until the TCP removal rate was stable, i.e., TCP removal rates were more than 80% for at least 2 weeks, which took about 2 weeks. For photodegradation-alone experiments, the bare (without any biofilm) ceramic honeycomb carrier was installed in the IPBR.

TCP degradation experiments

As a control, the IPBR was operated in batch without UV light and with no biofilm in the ceramic carrier. For three consecutive experiments, the initial TCP concentration was 17, 18, or 25 mg/l, and fresh ceramic was used in the first test corresponding to 18 mg/l, which lasted for 3 h. Then, the second and third control tests, respectively, corresponding to 17 and 25 mg/l, immediately followed the first to investigate if adsorption had been a factor in the first control test.

Three protocols were used to degrade TCP in batch experiments: photocatalysis (P), biodegradation (B), and intimately coupled photocatalysis and biodegradation (P&B). For the P and P&B experiments, the UV wavelength was 254 nm, the power was

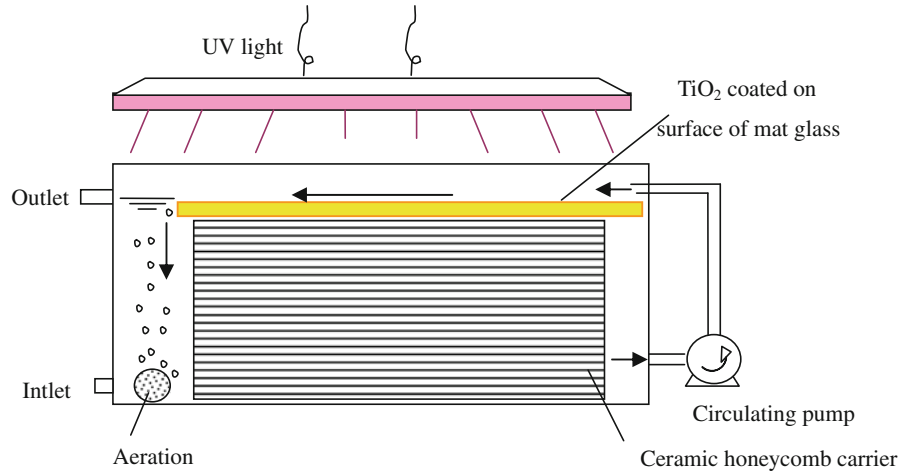

Fig. 1 Schematic of the integrated photocatalytic-biological reactor (IPBR)

24 W, the light intensity was 0.46 mW/cm^2, the distance between the UV light and the TiO_2 film was about 30 mm, and the depth of solution over the TiO_2 film was about 5 mm. The P experiments were carried out with the UV light turned on and no biofilm on the ceramic honeycomb carrier. For the B experiment, the ceramic honeycomb carrier with biofilm was installed in the reactor, and the UV light was turned off. During the P&B experiments, the ceramic honeycomb carrier with biofilm was used, and the UV light was turned on at the same time.

Sequentially and intimately coupled photodegradation and biodegradation were compared for degradation of 2,4,6-TCP. The sequential experiments were carried out in batch, and the process was divided into two phases, i.e., photodegradation followed by biodegradation. The sequential process was carried out in two ways that had a total treatment time of 5 h in each case: 2 h of photodegradation followed immediately by 3 h of biodegradation (P2+B3) and 3 h of photodegradation followed immediately by 2 h of biodegradation (P3+B2). After the P experiment, the bare carrier was immediately replaced by the biofilm-coated carrier, and the B experiment followed immediately. For direct comparison, intimately coupled P&B was carried out for 5 h in batch (P&B5).

During most batch experiments, TCP was diluted with tap water to which the inorganic salt components of the acclimation and incubation medium were added, and the initial TCP concentration was 5–30 mg/l.

For each batch experiment, 150 ml of solution containing 2,4,6-TCP was added to the IPBR; this was slightly more volume than the working volume and was used to compensate for the volume contained in the circulating pump and tubing and for the consumption of volume by sampling. The solution inside the IPBR was circulated over the TiO_2 film on mat glass and through the ceramic honeycomb carrier by the internal-circulation pump, and the circulation velocity was approximately 30 ml/min, and the retention time in the ceramic each cycle circulation was $V_{cer}/Q_{red} = 56$ s. The samples were taken from the top in the reactor at specified time intervals and assayed for the TCP concentration. The treated solution was discharged from the outlet after each experiment, and fresh solution was put into the reactor for another batch experiment.

In addition, batch experiments in which 200 mg/l of phenol was added (along with 20 mg/l of 2,4,,6-TCP) were carried out for 3 h in the P, B, and P&B modes. The goal of this series was to evaluate the possibility that mineralization of TCP and its photocatalysis products could be enhanced by means of secondary utilization (Aranda et al. 2003; Namkung and Rittmann 1987a,b). For these experiments, phenol alone and mixtures of phenol plus TCP were studied in parallel experiments to estimate the share of COD removal contributed by phenol in the mixed solution. The COD removal attributable to TCP was computed by difference.

Cl^- released from TCP

In order to measure the release of chloride ions during photocatalysis, a special P experiment utilized

20 mg/l (100 μM) 2,4,6-TCP dissolved in ultrapure water (18 MΩ) instead of tap water. This eliminated the large background Cl^- concentration, making it possible to detect Cl^- release, one sign of TCP mineralization. The solution containing TCP was treated with UV illumination for 300 min., and samples were taken at intervals to measure TCP and Cl^-.

Analytical methods

TCP was measured by a high performance liquid chromatograph (HPLC, model: Agilent 1100, USA) equipped with a diode array detector (DAD) with wavelength of 250 nm and ZORBAX SB-C18 column (5 μm, 4.6 × 150 mm). The mobile phase was a methanol:water solution (80:20, v/v), and the flow rate was 1 ml/min. The UV light intensity was measured by illuminometer (model: BG-2254, China). All samples were filtered through a 0.45 μm cellulose acetate membrane filter before analysis.

The COD concentration was determined using potassium dichromate oxidation according to standard procedures (American Public Health Association (APHA) 2001; Wei 2002) that involve providing a stoichiometric excess of potassium dichromate, strong acid and heating conditions, silver sulfate as a catalyst, and mercury sulfate to avoid the interference of chloride ion. The Cl^- anion was measured by ion chromatography with DIONEX (USA) model ICS-2100, and the separation column was IonPac AG18, 50 × 4 mm. The mobile phase (eluent) was KOH with a flow rate of 1.0 ml/min.

Results and discussion

Control experiments

As a control to evaluate TCP adsorption to the carrier, the first control experiment, lasting for 3 h, showed about 50% loss of TCP, as shown in Fig. 2. However, the second and third control experiments with the same reactor, respectively, starting with 17 and 25 mg/l TCP, showed no TCP removal. As the IPBR had neither biofilm nor TiO_2, the removal in the first control test was loss by adsorption to the reactor, mostly to the bare ceramic carrier. The lack of

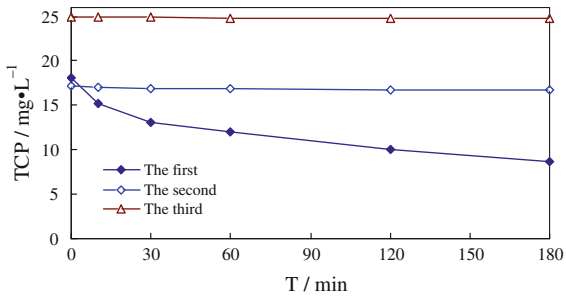

Fig. 2 Fate of TCP in three successive control experiments for evaluating TCP adsorption

removal in the second and the third tests indicates that the adsorption capacity was saturated by the first test. Because the ceramic carrier was reused for all following experiments, the adsorption phenomenon was unimportant for them.

Comparison of TCP removal rates by the different protocols

Figure 3 shows results for the batch-degradation kinetics with increasing initial TCP concentrations in P, B, and P&B experiments. TCP removal by P&B was the greatest for all initial TCP concentrations, and removal in P was greater than in B, although B showed significant removal. The advantage of the P&B protocol diminished for larger initial concentrations of TCP.

The results here differ from results when phenol was degraded by photobiodegradation in the IPBR (Zhang et al. 2010a,b), since chlorinated aromatics are much more difficult to biodegrade by microorganism alone due to their slow biodegradation kinetics and toxicity to the microorganisms (Marsolek and Rittmann 2007). Whereas photobiodegradation did not accelerate phenol removal in the earlier studies (Zhang et al. 2010a,b), photobiodegradation accelerated the TCP removal rates in this study, because TCP is much more slowly biodegraded.

Figure 4 shows the relationship between the initial TCP concentration and its initial removal rate (V_0) for the P, B, and P&B experiments; the initial rate is for the first 10 min. For the P experiments, V_0 increased gradually with increasing initial TCP concentration, while for the B experiments, V_0 increased gradually with increasing initial TCP concentration at first, but then decreased after 15 mg/l; the decline appears to

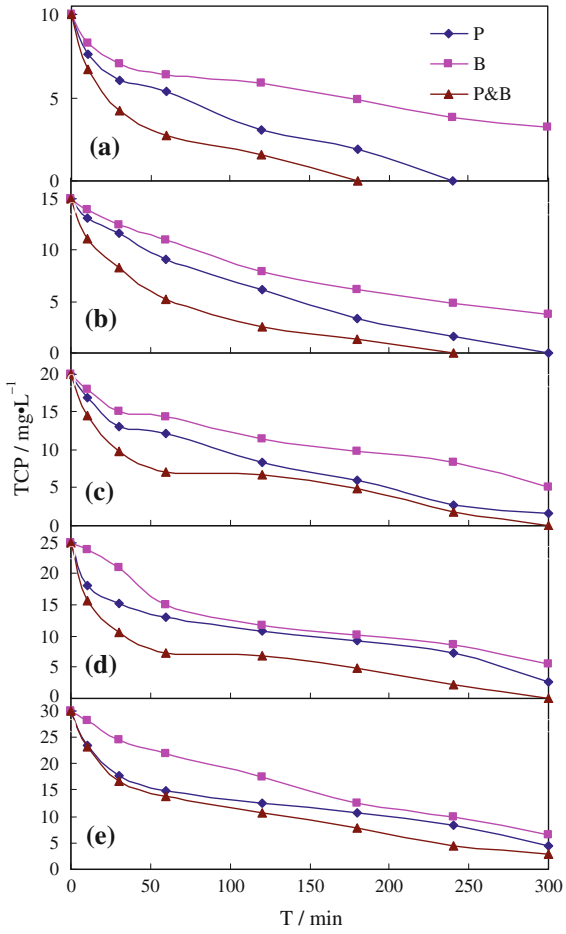

Fig. 3 TCP removal in batch experiments with different initial TCP concentrations by the P, B, and P&B protocols

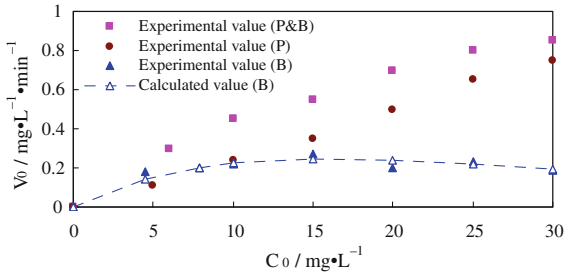

Fig. 4 Relationship between the initial TCP concentration and initial (first 10 min) removal rate (V_0)

be due to TCP inhibition to the microorganisms, which Marsolek and Rittmann (2007) showed to begin at a concentration around 10 mg/l. For the P&B experiments, V_0 increased with increasing initial TCP concentration up to 30 mg/l, an indication that

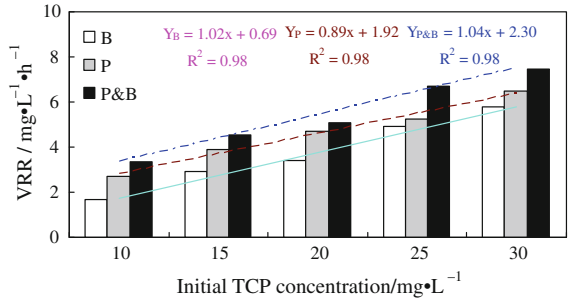

Fig. 5 TCP volumetric removal rates (VRR) for the first 180 min for the three batch protocols

photocatalytic degradation was important and that inhibition to biodegradation was overcome by intimate coupling to UV photocatalysis.

The kinetics for inhibited biodegradation can be represented by the Aiba equation (Aiba et al. 2000; Qi and Wang 2007):

$$V = \frac{V_{\max} C_S}{K_S + C_S} \exp\left(-\frac{C_S}{K_{SI}}\right)$$

in which V and $V_{\max}$ are, respectively, the TCP removal rate and the maximum removal rate; K_S and K_{SI} are, respectively, half-maximum-rate concentration and inhibition concentration; and C_S is the TCP concentration. This relationship can describe the volumetric TCP removal rate (V_0) in the first 10 min of the B experiments, since the biomass concentration did not change.

The three parameters were adjusted to fit the Aiba equation by means of trial and error method until all experimental data of the B experiment were represented well and the fit showed no systematic errors; these features are illustrated in Fig. 4. In addition, the R^2 value was high, 0.95. The parameter values are $V_{\max} = 2.8$ mg/l/min; $K_S = 66$ mg/l, and $K_{SI} = 20$ mg/l. The relatively low value of K_{SI} indicates that inhibition was important, and Fig. 4 shows that inhibition in the B experiments significantly lowered V_0 from what it would have been had inhibition not occurred.

Figure 5 presents the TCP volumetric removal rates for the first 3 h for the three protocols (i.e., VRR $= \Delta S/t$, in which ΔS is the difference of TCP concentration between the initial and final, and t is time of treatment, i.e., 180 min). The computation is for 3 h, because the TCP concentration became zero after 3 h in some experiments. The VRR by P&B was

the highest among the three protocols for all initial TCP concentrations, with P always faster than B. The three VRRs increased with increasing initial TCP concentration, and the slope by P&B is larger (1.04/h) than for B (1.02/h) and P (0.89/h). Here, the VRRs of the B experiments increased steadily with increasing initial TCP concentration. These trends further support that TCP inhibition to the biofilm was relieved when photocatalysis was intimately coupled with biodegradation. Similarly, Marsolek and Rittmann (2007) found that long-term incubation allowed aerobic microbial communities to degrade TCP due to gradual loss of inhibition, as long as the starting concentration was not too large (i.e., <40 μM for 2,4,5-TCP).

Comparison of intimately coupled with sequentially coupled photocatalysis and biodegradation of TCP

Figure 6 shows TCP removals by the three P&B protocols (influent = 20 mg/l): sequential P2+B3, sequential P3+B2, and intimate P&B5. The TCP degradation rate with P&B5 obviously was faster than that by P2+B3 and P3+B2, and, at the end of the 5 h batch experiments, TCP removal by P&B5 was 100%. The two sequential experiments gave the same removals for the first 120 min, since both were dominated by photocatalysis. P3+B2 gave greater TCP removal than P2+B3 at 180 min, since TCP removal initially was faster by photocatalysis. However, P2+B3 had better removal at the end of the experiment: 88 versus 77%. While this result suggests that long-term TCP removal was improved by switching to B earlier, the main conclusion from the comparison experiments is that P&B5 had superior TCP removal throughout the experiments.

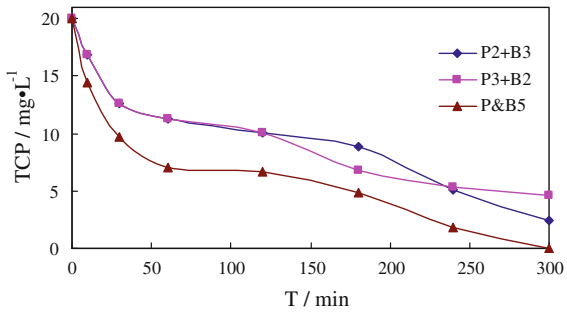

Fig. 6 Comparison of TCP degradation rate by sequentially and intimately coupled photocatalysis and biodegradation

The P&B5 experiment showed a trend of accelerating biodegradation after about 120 min. The acceleration of TCP loss may have been brought about by an increased rate of TCP biodegradation as TCP inhibition was relieved. The main conclusion from the comparison experiments is that P&B5 had superior TCP removal throughout the experiments.

Mineralization of TCP

COD removal is the index to measure the degree of TCP mineralization, but COD removal was minimal when TCP was the sole organic compound in the medium (data not shown here). Therefore, the experiments were repeated with 20 mg/l of TCP and 200 mg/l of phenol together, in order to promote TCP mineralization through secondary utilization (Aranda et al. 2003; Namkung and Rittmann 1987a,b). Experiments were carried out with 200 mg/l of phenol alone (giving 474 mg/l COD) and 200 mg/l phenol plus 20 mg/l TCP (giving 493 mg/l COD).

Figure 7 summarizes the results for phenol and TCP degradation. After 3 h with the mixed solution, 200 mg/l phenol declined to 174, 5.5, and 3.2 mg/l in P, B, and P&B experiments, respectively, (middle panel in Fig. 7). With the mixture of phenol and TCP, degradation of phenol was slower than with phenol alone in the B and P&B experiments, probably due to TCP inhibition. In the mixture experiment, the 20 mg/l TCP declined to 2.7, 0, and 0 mg/l in the P, B and P&B experiments, respectively. Comparing the TCP panel in Fig. 7 with Fig. 3c clearly shows that the TCP removal rate was faster when phenol was added for B and P&B with the same initial TCP concentration of 20 mg/l. This result supports a secondary utilization effect.

Figure 8 shows the COD removals. For the mixed solution, which had an initial COD of 493 mg/l, the COD removals were 80, 461, and 466 mg/l for P, B, and P&B experiments, respectively. COD removals contributed by phenol alone were 74, 447, and 448 mg/l from the starting COD of 474 mg/l. By difference, the COD removals for TCP degradation were 6, 14, and 18 mg/l for P, B, and P&B experiments, respectively. They constituted 32, 74, and 95% mineralizations of the 19 mg/l starting COD

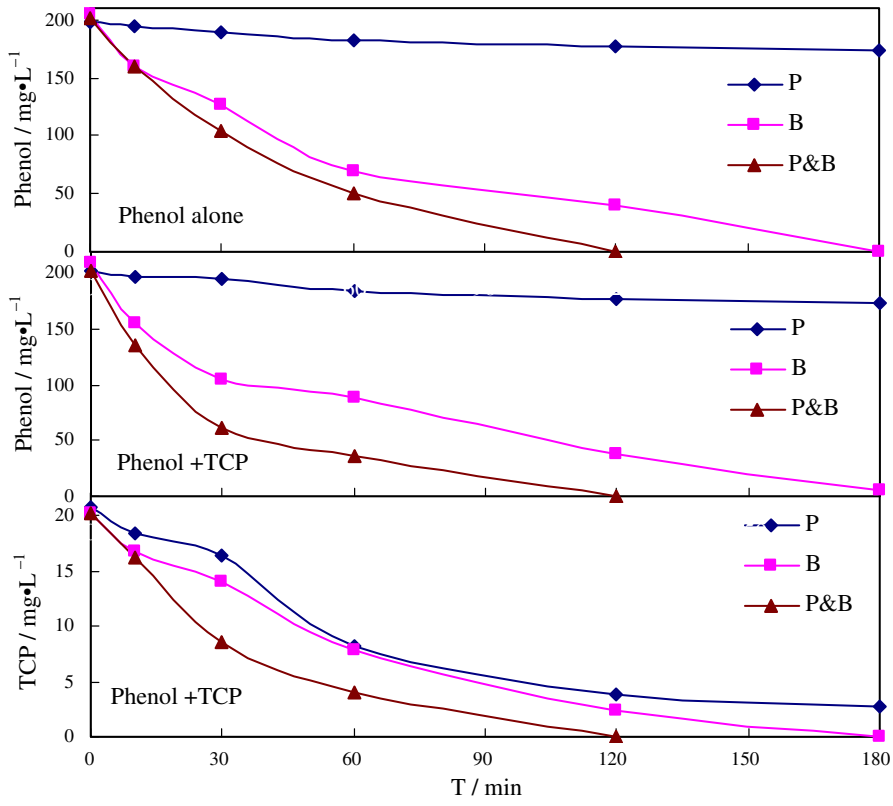

Fig. 7 Degradation of phenol with phenol alone (*top panel*) and of phenol and TCP together (*bottom two panels*) in P, B, and P&B batch experiments

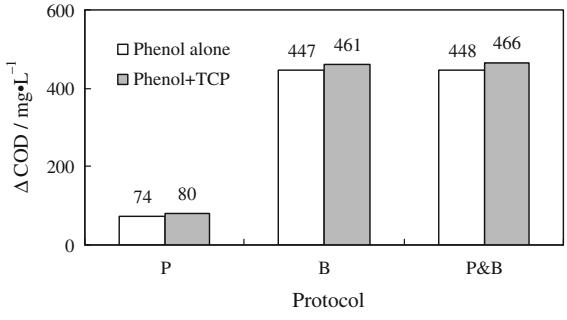

Fig. 8 COD removed for phenol alone and mixed phenol and TCP at 180 min

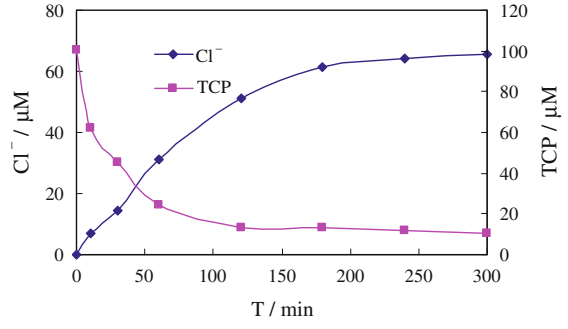

Fig. 9 Cl^- released from TCP and corresponding TCP removal with a P experiment in a chloride-free medium

of TCP. Similar to TCP loss, the benefits of P&B treatment and of secondary utilization are evident for mineralization.

Chloride anions release

Figure 9 shows Cl^- released in a special P experiment lasting 300 min in medium containing no other source of Cl^-. The Cl^- concentration increased steadily to 66 μM (2.3 mg/l) at the same time that the TCP concentration declined by 90 μM (17.8 mg/l). This corresponds to a release of 24% of the Cl contained on the removed TCP. Thus, 76% of the Cl remained bonded with the photocatalysis intermediates, although 89% of TCP was degraded. The findings on Cl^- release are consistent with only 32% mineralization by P (Fig. 8) and support that photocatalysis intermediates were not readily degraded by P alone.

Conclusions

TCP removal by intimately coupled photocatalysis and biodegradation was faster than that by photocatalysis or biodegradation alone. Degradation by photocatalysis was faster than by biodegradation when the TCP concentration was high enough to be inhibitory ($> \sim 15$ mg/l), and photocatalysis decreased the TCP concentration so that biodegradation could become more important over the long term. When compared directly, intimate coupling in P&B5 accelerated the TCP removal rate, compared to sequentially coupled P2+B3 and P3+B2.

TCP mineralization could be realized by adding phenol to promote secondary utilization, with P&B giving 95% mineralization of TCP at the end of the 180-min experiment. In comparison, the P and B experiments gave 32 and 74% mineralizations of TCP, respectively. Mineralization also was indicated by the Cl^- released from the ring in P experiments: Cl^- release was 24% when the degree of mineralization as 32% after 3 h of photocatalysis.

In summary, intimate coupling of photocatalysis and biodegradation in the IPBR made it possible to obtain the best features of each: rapid photocatalytic transformation in parallel with biological mineralization of photocatalytic products.

Acknowledgments The authors acknowledge the financial support by the National Natural Science Foundation of China (50978164 and 50678102), the Special Foundation of Chinese Colleges and Universities Doctoral Discipline (20070270003), Innovation Fund for Key Projects of Shanghai Municipal Education Commission (10ZZ82), the Shanghai Leading Academic Discipline Project (S30406), and the United States National Science Foundation (0651794). We received important help from Shanghai Application Lab, Dionex China Co., Ltd. for Cl^- anion measurement.

References

Agrios AG, Gray KA, Weitz EK (2004) Narrow-band irradiation of a homologous series of chlorophenols on TiO_2: charge-transfer complex formation and reactivity. Langmuir 20(14):5911–5917

Aguedach A, Brosillon S, Norvan J, Lhadi EK (2005) Photocatalytic degradation of azo-dyes reactive black 5 and reactive yellow 145 in water over a newly deposited titanium dioxide. Appl Catal B Environ 57(1):55–62

Aiba S, Shoda M, Nagalani M (2000) Kinetics of product inhibition in alcohol fermentation. Biotechnol Bioeng 67(6):671–690

Ali M, Sreekrishnan TR (2001) Aquatic toxicity from pulp and paper mill effluents: a review. Adv Environ Res 5(2):175–196

American Public Health Association (APHA) (2001) Standard methods for the examination of water and wastewater, 22nd edition USA. American Water Works Association and Water Pollution Control Federation, Washington DC

Aranda C, Godoy F, Becerra J, Barra R, Martínez M (2003) Aerobic secondary utilization of a non-growth and inhibitory substrate 2, 4, 6-trichlorophenol by *Sphingopyxis chilensis* S37 and *Sphingopyxis*-like strain S32. Biodegradation 14(4):265–274

Chan CY, Tao S, Dawson R, Wong PK (2004) Treatment of atrazine by integrating photocatalytic and biological processes. Environ Pollut 131(1):45–54

Chu W, Wong CC (2003) A disappearance model for the prediction of trichlorophenol ozonation. Chemosphere 51(4):289–294

Häggblom MM (1992) Microbial breakdown of halogenated aromatic pesticides and related-compounds. FEMS Microb Rev 103(1):29–72

Han WY, Zhu WP, Zhang PY, Zhang Y, Li LS (2004) Photocatalytic degradation of phenols in aqueous solution under irradiation of 254 and 185 nm UV light. Catal Today 90(3–4):319–324

Hess TF, Lewis TA, Crawford RL, Katamneni S, Wells JH, Watts RJ (1998) Combined photocatalytic and fungal treatment for the destruction of 2, 4, 6–trinitrotoluene (TNT). Water Res 32(5):1481–1491

Juhl U, Blum JK, Butte W, Witte I (1991) The induction of DNA strand breaks and formation of semiquinone radicals by metabolites of 2, 4, 5-trichlorophenol. Free Radic Res Commun 11(6):295–305

Marsolek MD (2005) Photobiocatalysis: coupled photocatalytic-biologic treatment for recalcitrant and inhibitory wastewaters. Dissertation for the degree of PhD Northwestern University, Evanston

Marsolek MD, Rittmann EB (2007) Biodegradation of 2, 4, 5-trichlorophenol by mixed microbial communities: biorecalcitrance, inhibition, and adaptation. Biodegradation 18(3):351–358

Marsolek MD, Torres CI, Hausner M, Rittmann EB (2008) Intimate coupling of photocatalysis and biodegradation in a photocatalytic circulating-bed biofilm reactor. Biotechnol Bioeng 101(1):83–92

Mohanty S, Rao NN, Khare P, Kaul SN, Mohanty S (2005) A coupled photocatalytic–biological process for degradation of 1-amino-8-naphthol-3, 6-disulfonic acid (H-acid). Water Res 39(20):5064–5070

Namkung E, Rittmann BE (1987a) Modeling bisubstrate removal by biofilms. Biotechnol Bioeng 29(2):269–278

Namkung E, Rittmann BE (1987b) Evaluation of bisubstrate secondary utilization kinetics by biofilms. Biotechnol Bioeng 29(3):335–342

National Cancer Institute (NCI) (1979) Bioassay of 2,4,6-trichlorophenol for possible carcinogenicity. NIH Publication No. 79-1711 National Cancer Institute, Bethesda

Parra S, Malato S, Pulgarin C (2002) New integrated photocatalytic-biological flow system using supported TiO_2 and fixed bacteria for the mineralization of isoproturon. Appl Catal B Environ 36(2):131–144

Qi Y, Wang S (2007) Biological reaction kinetics and reactor, 3rd edn. Chemical Industry Press, Beijing

Stafford U, Gray KA, Kamat PV (1994) Radiolytic and TiO2-assisted photocatalytic degradation of 4-chlorophenol–a comparative study. J Phys Chem 98(25):6343–6351

Stafford U, Gray KA, Kamat PV (1997) Photocatalytic degradation of 4-chlorophenol: the effects of varying TiO_2 concentration and light wavelength. J Catal 167(1):25–32

Wei F (2002) Monitoring and analytic methods of water and wastewater, 4th edn. Environmental Science Press of China, Beijing

Zhang Y, Han L, Wang J, Yu J, Shi H, Qian Y (2002a) An internal airlift loop bioreactor with *Burkholderia pickttii* immobilized onto ceramic honeycomb support for degradation of quinoline. Biochem Eng J 11(2–3):149–157

Zhang ZS, Anderson WA, Moo-Young M (2002b) Photocatalytic pretreatment of contaminated groundwater for biological nitrification enhancement. J Chem Technol Biotechnol 77(2):190–194

Zhang Y, Quan X, Rittmann EB, Wang J, Shi H, Qian Y, Yu J (2004) IAL-CHS (internal airlift loop–ceramic honeycomb supports) reactor used for biodegradation of 2, 4-dichlorophenol and phenol. Water Sci Technol 49(11–12): 247–254

Zhang Y, Wang L, Rittmann EB (2010a) Integrated photocatalytic-biological reactor for accelerated phenol degradation. Appl Microb Biotechnol 86(6):1977–1985

Zhang Y, Liu H, Shi W, Pu X, Rittmann EB (2010b) Photobiodegradation of phenol with ultraviolet irradiation of new ceramic biofilm carriers. Biodegradation 21(6): 881–887